0026-895X/89/030360-09$02.00/0

MOLECULAR PHARMACOLOGY, 35:360-368

N-Methyl-D-Aspartate/Glycine and Quisqualate/Kainate Receptors Expressed in *Xenopus* oocytes: Antagonist Pharmacology.

TODD A. VERDOORN,[1] NANCY W. KLECKNER, and RAYMOND DINGLEDINE

Department of Pharmacology and Curriculum in Neurobiology, University of North Carolina, Chapel Hill, North Carolina 27599

Received September 18, 1988; Accepted December 5, 1988

SUMMARY

Quantitative pharmacological studies were done to determine the properties of excitatory amino acid receptors expressed in *Xenopus* oocytes injected with rat brain mRNA. Smooth currents with properties indicative of *N*-methyl-D-aspartate (NMDA) and quisqualate/kainate receptors were observed in mRNA-injected oocytes. Schild analysis of currents evoked by NMDA indicated that the EAA receptor antagonist D-2-amino-5-phosphonovalerate (D-APV) exerted a competitive block of the oocyte NMDA receptor, because the Schild regression was linear with a slope not significantly different from unity (1.03 ± 0.025) up to 100 μM D-APV. The pA_2 estimated for D-APV antagonism of NMDA currents (5.87 ± 0.043) was nearly identical to that for D-APV as an L-aspartate antagonist (pA_2 = 5.86 ± 0.073, slope = 0.97 ± 0.036), suggesting that these two agonists are selective for NMDA receptors in oocytes up to concentrations well above 1 mM. 6-Nitro-7-cyano-quinoxaline-2,3-dione (CNQX) reduced the maximum NMDA response significantly (70% reduction by 15 μM CNQX) but had no effect on the NMDA EC_{50}. CNQX exerted a mixed competitive-noncompetitive block of the glycine site on NMDA receptors; 15 μM CNQX increased the glycine EC_{50} by 5-fold and reduced the maximum glycine response by 35%. In addition, CNQX exerted a potent and competitive antagonism of currents evoked by kainate. The Schild regression was linear up to 30 μM CNQX with a slope of 1.02 ± 0.014 and a pA_2 of 6.53 ± 0.029. The block of kainate or NMDA currents by 2 μM CNQX was not voltage dependent. D-APV exerted a weak antagonism of kainate-evoked currents, with a pA_2 of 3.39 ± 0.044, but the slope of the Schild regression was slightly less than 1 (0.90 ± 0.03). These data demonstrate a clear pharmacological distinction between receptors that mediate the kainate- and NMDA-induced currents and quantify the potency of CNQX and D-APV acting at NMDA/glycine and quisqualate/kainate receptors. The implications of these data for the identification of EAA receptors in oocytes and the classification of neuronal EAA receptors are discussed.

Since the original classification scheme for EAA receptors was proposed by Watkins and Evans (1), multiple attempts have been made to confirm quantitatively the three EAA receptor hypothesis. The classification schemes of other neurotransmitter receptors (e.g., the cholinergic and adrenergic systems) are based on quantitative comparisons of antagonist potency. However, analogous information is unavailable for the EAA receptors because there are few known antagonists that clearly distinguish among each of the putative EAA receptor types. Greater complexity of EAA receptor function revealed in recent single-channel studies (2–6) and a burgeoning interest in the development of new therapeutic agents that act on EAA receptors increase the need for a rational classification scheme based on quantitative comparisons of antagonist potency.

NMDA receptors can be distinguished from other EAA receptors by the actions of a number of selective competitive (7–10) and uncompetitive (11–13) antagonists. The potencies of the competitive NMDA receptor antagonist D-APV and its racemic mixture DL-APV range from 1.4 to 12 μM (7–9, 14–16). The varying potency estimates might imply heterogeneous populations of D-APV-sensitive NMDA receptors, as might the apparently different effects of D-APV on neuronal depolarizations evoked by quinolinate and ibotenate (14, 17).

The kainate and quisqualate receptors (1) are not as easily differentiated from each other. Antagonists that distinguish between kainate- and quisqualate-evoked excitation are not yet available, and it has not been possible to demonstrate the existence of two non-NMDA EAA receptors that mediate neuronal depolarization. A number of antagonists have been tested,

This work was supported by Grants NS-17771 and NS-22249 and a Predoctoral Fellowship from the Pharmaceutical Manufacturers' Association Foundation (T.A.V.).

[1] Present address: Max-Planck-Institut fur biophysikalishe Chemie, D-3400 Gottingen, Federal Republic of Germany.

ABBREVIATIONS: EAA, excitatory amino acid; NMDA, *N*-methyl-D-aspartate; APV, 2-amino-5 phosphonovalerate; DNQX, 6,7-dinitroquinoxaline-2,3-dione; CNQX, 6-nitro-7-cyano-quinoxaline-2,3-dione; MBS, modified Barth's solution; AMPA, α-amino-3-hydroxy-5-methylisoxazole-4-propionic acid.

such as γ-D-glutamylglycine (18), γ-D-glutamylaminomethylsulfonate (19), kynurenate (20, 21), and derivatives of piperazine-2,3-dicarboxylic acid (22). However, these compounds have low potency and significant antagonist activity against all three EAA agonists (19–22). The most potent non-NMDA receptor antagonists yet tested are the quinoxalinediones DNQX and CNQX. Neither of these compounds strongly distinguishes between the effects of kainate and quisqualate, and they show substantial antagonism of NMDA receptors (23). Therefore, if the limited armentarium of available compounds persists, demonstration of the number and properties of EAA receptors will likely require quantitative studies in which small differences can be reliably detected.

Unfortunately, central nervous tissue is not well suited to quantitative pharmacological studies. Particularly problematic is the difficulty in controlling and manipulating the chemical environment at the receptors. Slow diffusion, uptake, and degradation of applied compounds coupled with the possibility of release of endogenous agonists, antagonists, and modulators of EAA receptors compromise the results of pharmacological analyses in intact tissues. With the exception of uptake (24), the effect of these processes on pharmacological characterization of EAA receptors has not been studied. The *Xenopus* oocyte mRNA translation system provides a preparation that is more amenable to experimental control because the effects of diffusion, uptake, release, and degradation can be minimized. We have previously shown that currents with properties expected from activation of NMDA and quisqualate/kainate receptors are seen in mRNA-injected oocytes (25–27). We have reported the relative potencies of a number of agonists that act on these receptors (26). In order to determine more precisely the identity of the receptors mediating the EAA-evoked smooth currents in oocytes, we have quantified the effects of D-APV and CNQX on currents evoked by NMDA/glycine, L-aspartate, and kainate. A preliminary report of some these results has appeared (28).

Materials and Methods

The methods for mRNA preparation, culture, injection, and voltage clamp of oocytes were essentially as previously described (26). Briefly, RNA was isolated from fresh rat brain tissue by homogenizing the tissue in 4 M guanadinium thiocyanate and centrifuging the homogenate over 5.7 M CsCl at 83,000 × *g* for 18 hr at 20°. The RNA pellet was extracted with phenol/chloroform and poly A$^+$ mRNA was selected by one round of oligo-dT cellulose chromatography. The mRNA was dissolved in water at a final concentration of 0.8–1.2 mg of RNA/ml and 50–75 nl of this solution was injected into each oocyte. Before injection, oocytes were shaken gently in a solution of 1–2 mg/ml neutral dispase (Boeringer Mannheim, Indianapolis, IN) in MBS for 1 hr, and some oocytes were then manually defolliculated after shrinking in MBS made hyperosmotic with sucrose. When glycine was studied, oocytes were always defolliculated to minimize diffusion barriers and prevent release of endogenous glycine agonists from follicle cells. The oocytes were cultured in MBS supplemented with 0.01 mg/ml each of penicillin and streptomycin for at least 48 hr before being voltage clamped at −60 mV. Agonists were dissolved in MBS and applied by perfusion until a steady maximum response amplitude was reached for each concentration. Currents evoked by agonists were filtered at 20 Hz and measured from digitized records on an IBM AT computer.

Agonist concentration-response curves were determined as described (26). The maximum response amplitude, the agonist concentration causing half-maximal response (EC_{50}), and a slope coefficient (n) were estimated for each curve by fitting the data to the logistic equation:

$$\text{amplitude} = \text{maximum amplitude}/[1+(EC_{50}/[\text{agonist}])^n]$$

with a nonlinear least squares curve-fitting program. Antagonist potencies were determined by Schild analysis (29). For Schild analysis of quisqualate/kainate receptors, the maximum response in a particular cell was determined by perfusing 1 mM kainate; this response amplitude was stable for several hours (Fig. 1). For Schild analysis of NMDA receptors, the maximum was not determined in this way because the current elicited by a saturating concentration (300 μM) of NMDA often decreased gradually over 2 hr (Fig. 1). In contrast, the response evoked by 10 μM NMDA remained relatively stable. This rundown phenomenon is similar to that found in cultured hippocampal neurons (30). For NMDA and L-aspartate, the maximum response amplitude was interpolated from responses evoked by high concentrations of agonist (300 μM) during the washout periods between each antagonist application.

Three concentrations of agonist were applied under control conditions (no antagonist) for a time sufficient to allow the current to reach a steady value. Antagonists were then perfused for at least 5 min before three concentrations of agonist were applied in the presence of antagonist. Agonists and antagonists were applied from low to high concentration. Agonist concentrations were chosen to assure that the half-maximal response level was bracketed in each concentration of antagonist. Dose-ratios were calculated at the EC_{50} response level, which was determined by interpolation of a linear regression of fractional response versus the log of the agonist concentration. The pA_2 and slope were determined for each cell by linear regression of the Schild plot and the mean values and standard errors of each separate determination are reported here.

Results

The responses evoked by NMDA and L-aspartate were often biphasic, with a sharp initial response followed by a slowly rising late current. D-APV blocked both phases equally (Fig. 2A) and the NMDA reversal potential during the first phase (−7 ± 4 mV; n = 4) was identical to that measured late in the response in the same cell (−7 ± 2 mV). The initial sharp response was somewhat variable within a given cell and may have been influenced by perfusion speed, so the amplitudes of

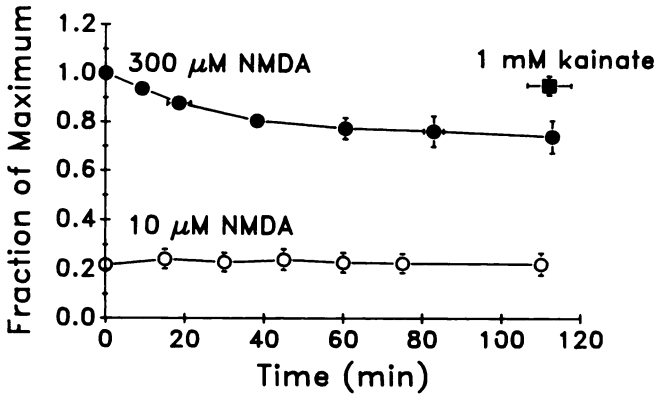

Fig. 1. Rundown of the maximum NMDA-induced current over time. The amplitude of currents evoked by 10 μM (○) and 300 μM (●) NMDA relative to the initial maximum response is plotted as a function of time after the initial application. The 10 μM *points* represent the mean ± standard error of four experiments in which 10 μM and 300 μM NMDA were presented alternately in pairs. Ten minutes separated the application of each pair of concentrations whereas 5 min separated the applications of concentrations within a pair. The last pair was applied 35 min after the previous pair. The 300 μM *points* represent the mean ± standard error of 10 experiments. *Error bars* for the *x* axis are included for these points because the time of application varied. The glycine concentration was 3 μM throughout. For comparison, ■ represents the relative amplitude of kainate-induced current determined during other experiments (n = 8).

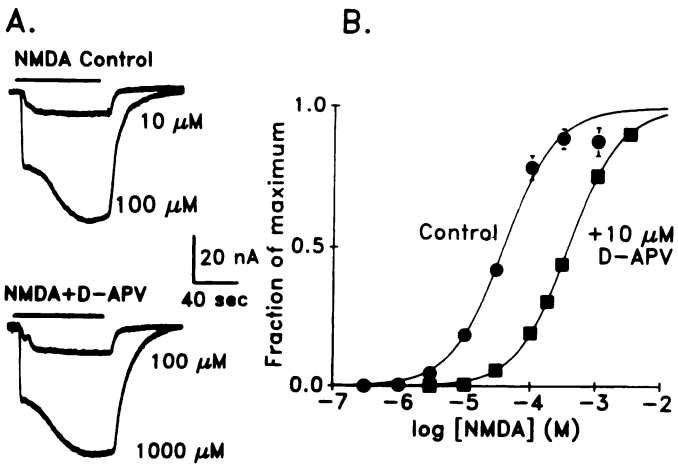

Fig. 2. D-APV shifts the NMDA concentration-response curve to the right in a parallel fashion. A, Examples of NMDA-evoked currents at −60 mV (no Mg^{2+}, 3 μM glycine) under control conditions (*top*) and in the presence of 10 μM D-APV (*bottom*). The concentration of NMDA denoted to the *right* of each trace was perfused during the time indicated by the *bars* above each set of traces. B, NMDA concentration-response curves under control conditions (●) and in the presence of 10 μM D-APV (■). Each *point* is the mean ± standard error of six separate oocytes in which two full concentration-response curves were constructed. The NMDA EC_{50} was shifted by approximately 11-fold, but the maximum response amplitude was unaffected. The effects of rundown were taken into account by alternating the order in which the concentration-response curves were constructed. Thus, the concentration-response curve in the presence of D-APV was done first in three cells and second in the other three.

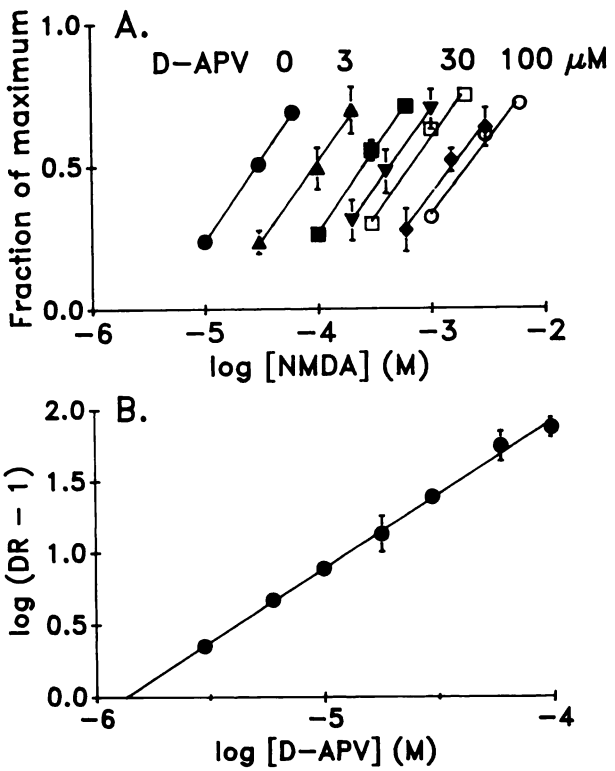

Fig. 3. Schild analysis of the antagonism by D-APV of currents produced by NMDA in mRNA-injected oocytes. A, Partial NMDA concentration-response curves in the presence of increasing concentrations (0, 3, 10, 20, 30, 60, and 100 μM) of D-APV. Each *point* represents the mean ± standard error of three to nine determinations. The maximum response amplitude elicited by 300 μM NMDA was tested before and after the construction of each curve. The mean amplitude of the bracketing test doses was used as the maximum response for a particular curve. B, Schild regression derived from the data illustrated in A. The *points* are the mean ± standard error of three to six determinations, with the exception of the *point* at 6 μM D-APV, which is a single observation. The *solid line* represents the regression over the pooled data ($n = 28$); the regression was highly significant ($p < 0.001$). The average slope of nine separate determinations was 1.03 ± 0.02 and the mean pA_2 was 5.87 ± 0.043. The glycine concentration was 3 μM throughout.

NMDA currents were measured during the late phase. The nature of the biphasic NMDA response requires further study.

D-APV

Antagonism of NMDA-induced currents. D-APV competitively blocked inward currents elicited by NMDA in mRNA-injected oocytes. The NMDA concentration-response curve was shifted to the right in a parallel fashion by 10 μM D-APV (Fig. 2B). In the absence of D-APV, the NMDA EC_{50} was 30.1 μM (95% confidence interval, 24.7–36.6 μM; n =6) whereas, in the presence of 10 μM D-APV, the average EC_{50} was 343 (272–435) μM in these six oocytes. D-APV did not change the maximum response (78.5 ± 15.6 nA in control versus 87.5 ± 21.0 nA in D-APV; $n = 6$), but the Hill coefficient was slightly lower in the presence of D-APV (mean = 1.19 ± 0.07) than under control conditions (mean = 1.38 ± 0.08; $p < 0.05$ by a two-tailed paired t test; $n = 6$).

Schild analysis (29) was performed to determine the potency of D-APV at NMDA receptors in oocytes and to verify the competitive nature of the D-APV block over a wider range of antagonist concentrations. A composite Schild plot obtained with data from nine cells and seven concentrations of D-APV is illustrated in Fig. 3. Fig. 3A shows that the NMDA concentration-response curves were shifted to the right in a parallel fashion, even up to 100 μM D-APV. The Schild regression (Fig. 3B) was linear, with an average slope of 1.03 ± 0.02, consistent with competitive antagonism, up to a mean dose ratio of 75.4 ± 10.8 ($n = 3$) produced by 100 μM D-APV. The average pA_2 determined in nine cells was 5.87 ± 0.04, which corresponds to an estimated K_B of 1.35 (1.11–1.64) μM for block of NMDA receptors by D-APV.

Antagonism of L-aspartate-induced currents. The currents evoked by L-aspartate in oocytes are blocked by Mg^{2+} in a voltage-dependent manner (26), suggesting that at EC_{50} concentrations L-aspartate activates mostly NMDA receptors in oocytes. To determine the selectivity of L-aspartate more quantitatively, Schild analysis of the antagonism of L-aspartate responses by D-APV was carried out for comparison with NMDA. A linear Schild plot (Fig. 4) with a slope of unity (0.97 ± 0.04; $n = 5$) indicated that D-APV also competitively blocked L-aspartate currents in oocytes. The dose ratio produced by 100 μM D-APV was 61.2 ± 14.7 ($n = 3$), and the pA_2 was 5.86 ± 0.07. The D-APV K_B values for blocking NMDA- and L-aspartate-induced currents were identical, suggesting that NMDA, L-aspartate, and D-APV act at the same receptor in oocytes.

Antagonism of kainate-induced currents. D-APV inhibited currents evoked by kainate in oocytes, although it appeared to be 295-fold less potent at these receptors than at NMDA receptors (Fig. 4). The average pA_2 determined for D-APV antagonism of kainate-induced currents was 3.39 ± 0.04 (n = 6). The Schild plot was linear up to 4 mM D-APV (agonist dose ratio = 9.15 ± 1.07; $n = 3$); however, the slope of the Schild regression (0.90 ± 0.03) was slightly but significantly ($p < 0.02$, two-tailed t test) less than 1. These data constitute strong

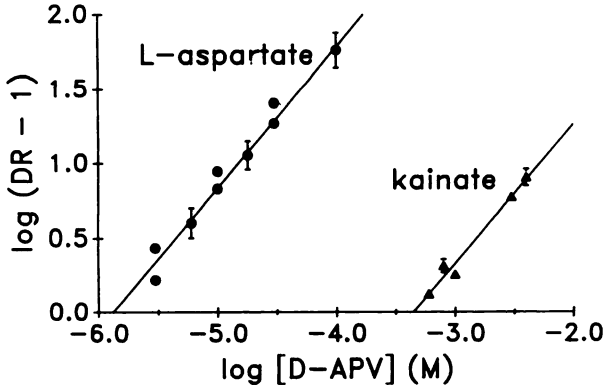

Fig. 4. Schild regressions of the D-APV antagonism of currents produced by L-aspartate (●) and kainate (▲). The *circles* represent the mean ± standard error for three determinations in the cases where *error bars* are present. Where no *error bars* are seen, the *points* are derived from single observations. For kainate, all *points* are the mean ± standard error of three separate determinations. The slopes of each *line* were linear and the regressions highly significant [L-aspartate slope = 0.972 ± 0.036 (n = 5), $p < 0.001$; kainate slope = 0.903 ± 0.031 (n = 6), $p < 0.01$]. The relative pA_2 [L-aspartate = 5.86 ± 0.073 (n = 5) versus kainate = 3.39 ± 0.044 (n = 6)] indicate D-APV is 295 times less potent at the receptor mediating the kainate current than it is at NMDA receptors. Glycine was set at 3 μM and Mg^{2+} was omitted when L-aspartate was studied.

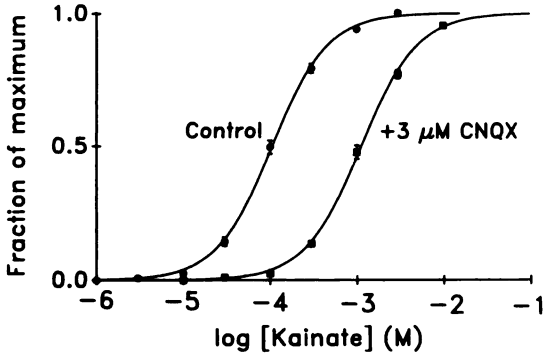

Fig. 5. Concentration-response curves for kainate in the presence and absence of 3 μM CNQX. Each *point* represents the mean ± standard error of five experiments in which complete concentration-response curves were constructed under both conditions. The kainate EC_{50} was shifted 10.6-fold to the right by 3 μM CNQX, whereas the maximum response and Hill coefficient were unaffected by the antagonist.

evidence that the receptors mediating kainate currents in mRNA-injected oocytes are different from those activated by NMDA and L-aspartate.

CNQX

Antagonism of kainate-induced currents. CNQX exerted a competitive block of kainate-evoked currents in oocytes, as demonstrated by a parallel shift to the right of the kainate concentration-response curve caused by 3 μM CNQX (Fig. 5). Complete concentration-response curves were constructed under control conditions and in the presence of 3 μM CNQX in five oocytes. The kainate EC_{50} was shifted from 106 (88.6–126) μM to 1120 (951–1320) μM by CNQX. Neither the Hill coefficient (1.37 ± 0.02 in control, 1.35 ± 0.03 in 3 μM CNQX; n = 5) nor the maximum response amplitude (204 ± 35.9 nA in control, 203 ± 35.0 nA in 3 μM CNQX; n = 5) was affected by the presence of antagonist.

The results of Schild analysis were completely consistent with a competitive mode of action for CNQX on the receptor mediating the kainate current in oocytes (Fig. 6). The Schild regression was linear, with a mean slope of 1.02 ± 0.01 (n = 19) up to an average dose ratio of 113 ± 16.3 produced by 30 μM CNQX (n = 3). The average pA_2 found for 19 cells was 6.53 ± 0.03. These data indicate that CNQX is the most potent competitive antagonist of non-NMDA receptors yet tested, with a K_B of 295 (259–336) nM.

CNQX did not appear to influence features of the kainate response other than agonist potency. The block of kainate currents by CNQX was not dependent on membrane potential (Fig. 7A). In five cells tested in the presence and absence of CNQX, the reversal potential for the current evoked by 300 μM kainate was the same, −11 ± 1 mV under control conditions and −11 ± 2 mV in the presence of 2 μM CNQX. Moreover, CNQX did not significantly affect the ratio of the kainate chord conductances measured at +20 and −70 mV (control $G_{(+20)}/G_{(-70)}$ = 0.84 ± 0.04, 2 μM CNQX = 0.93 ± 0.13; n = 5). CNQX thus appeared to block the receptor mediating kainate currents without interfering with the conductance mechanism.

Antagonism of NMDA receptors at the glycine site. In contrast to the competitive block of kainate-evoked currents, CNQX blocked NMDA-induced currents noncompetitively (Fig. 8). In the presence of 3 μM glycine, full NMDA concentration-response curves were constructed with and without 6 or 15 μM CNQX. The maximum amplitude of the NMDA response was reduced from 83 ± 33 nA to 44 ± 14 nA by 6 μM CNQX (n = 3) and, in a separate group of oocytes, 15 μM CNQX decreased the maximum from 160 ± 31 nA to 49 ± 2.0 nA (n = 3). Whereas 6 μM CNQX shifted the kainate EC_{50} by an average of 26-fold (n = 7), the NMDA EC_{50} was not affected by the presence of this antagonist. Under control conditions the NMDA EC_{50} was 29.2 (23.5–36.3; n = 6) μM; in 6 μM CNQX

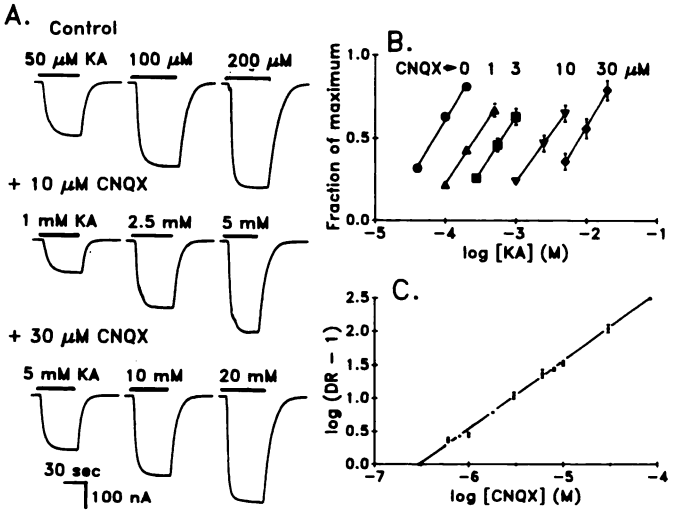

Fig. 6. Schild analysis of the antagonism of kainate-evoked currents by CNQX. A, Examples of inward currents produced by application of kainate during the times indicated by the *bars*, under control conditions (*top*) and in the presence of 10 μM (*middle*) and 30 μM (*bottom*) CNQX. The holding potential was −60 mV. B, Partial kainate concentration-response curves in the presence of increasing CNQX concentrations (indicated *above* each curve). Each *point* is mean ± standard error of 3 to 19 separate experiments. C, Schild regression derived from experiments partially illustrated in A and B. Each *point* represents the mean ± standard error of three to six determinations. The regression over the entire data set (*solid line*, n = 55) is highly significant ($p < 0.001$). The average slope of 19 separate experiments was 1.02 ± 0.02 and the mean pA_2 was 6.53 ± 0.029.

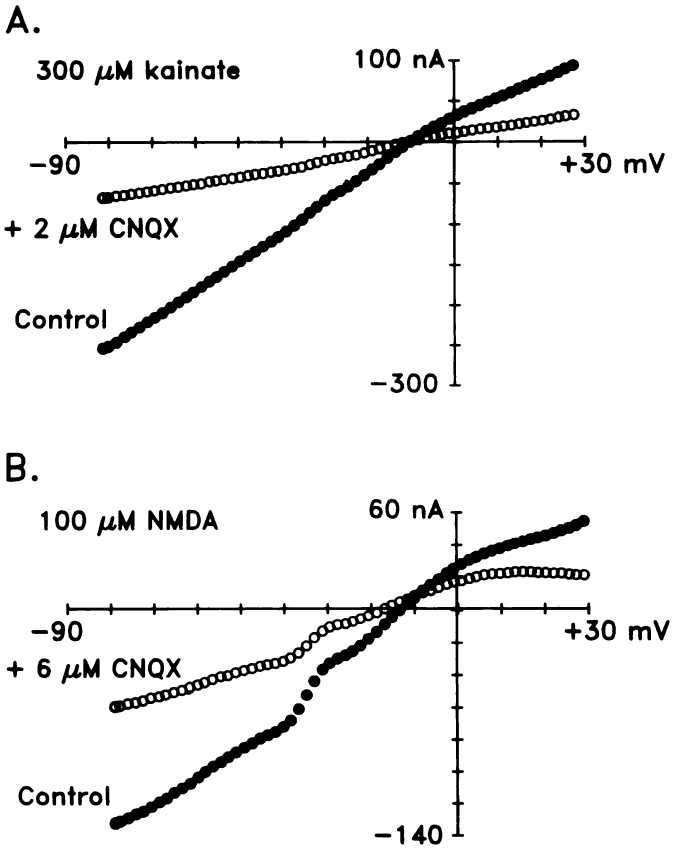

Fig. 7. The block by CNQX of currents evoked by kainate and NMDA is not voltage dependent. Current-voltage curves for the responses evoked by 300 μM kainate (A) and 100 μM NMDA plus 3 μM glycine (B) were constructed under control conditions (●) and in the presence of the indicated concentration of CNQX (○). CNQX did not affect the voltage dependency or reversal potential of either response.

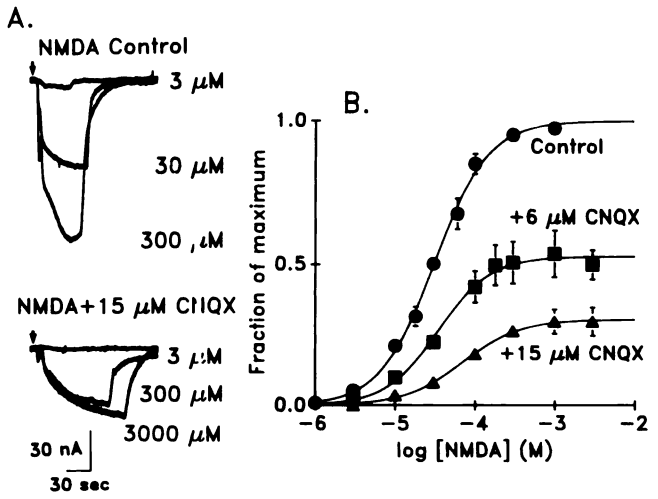

Fig. 8. Noncompetitive block of NMDA-induced inward currents by CNQX. A, Examples of currents evoked by application of NMDA (concentrations denoted on the *right*) starting at the time indicated by the *arrow* in the same mRNA-injected oocyte. The *top* set of traces shows the NMDA current under control condition, whereas the *bottom* illustrates the NMDA responses in the presence of 15 μM CNQX. B, Full NMDA concentration-response curves produced in the absence of antagonist (●) and in the presence of 6 μM (■) or 15 μM (▲) CNQX. The *control points* represent the mean ± standard error of six cells tested, whereas the *antagonist points* were derived from the mean ± standard error of three cells each. The *curves* are the results of nonlinear least squares fit of the data to the logistic equation and are plotted relative to the maximum current determined in the absence of antagonist. Glycine was 3μM throughout.

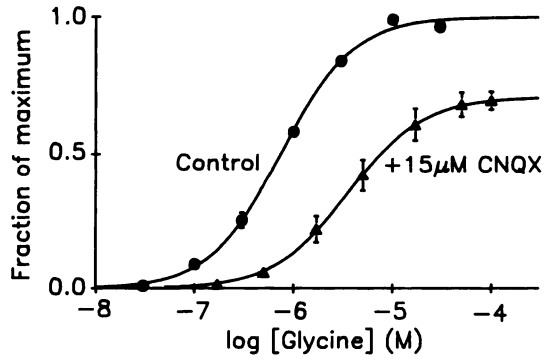

Fig. 9. Mixed competitive-noncompetitive block by CNQX of the glycine site on NMDA receptors. Oocytes were exposed to increasing concentrations of glycine in the presence of fixed 100 μM NMDA, with and without 15 μM CNQX. The *points* represent the mean ± standard error from five oocytes. The *curves* are the results of nonlinear least squares fit of the data to the logistic equation and are plotted relative to the maximum current determined in the absence of CNQX.

it was 35.0 (34.5–35.6; $n = 3$) μM, and in 15 μM CNQX it was 70.5 (37.9–131; $n = 3$) μM. The differences between the NMDA EC_{50} values under each of these conditions were not statistically significant (two-tailed paired t tests).

CNQX did not appear to alter the NMDA conductance (Fig. 7B), inasmuch as it did not change the NMDA reversal potential (−12 ± 2 mV in control, −15 ± 2 mV in 6 μM CNQX; n = 5) nor did it significantly affect the NMDA chord conductance ratio measured in the absence of Mg^{2+} ($G_{-60}/G_{(-30)}$ = 0.94 ± 0.094 in control and 0.82 ± 0.094 with 6 μM CNQX; $n = 5$).

The noncompetitive block of NMDA currents by CNQX suggested that this antagonist might act at the glycine recognition site of NMDA receptors (6, 25, 27, 31). This idea was borne out by concentration-response studies of glycine carried out in the presence of a fixed (100 μM) concentration of NMDA. The glycine EC_{50} was increased from 0.74 (0.64–0.87) μM to 3.87 (2.44–6.12) μM by 15 μM CNQX, but the maximum response was also reduced by 35% (Fig. 9). The antagonism of NMDA receptors by CNQX, therefore, appears to be purely noncompetitive for NMDA and to be mixed competitive-noncompetitive for glycine.

Effects on other agonist-induced currents. Although different mechanisms of action were apparent, CNQX was effective at inhibiting smooth currents produced by activation of both NMDA and non-NMDA receptors in oocytes. Smooth currents evoked by approximately EC_{50} concentrations of kainate, NMDA, AMPA, L-aspartate, D-aspartate, and L-glutamate were all significantly reduced by 10 μM CNQX (Fig. 10; Table 1). Although CNQX potently blocked quisqualate-induced neuronal depolarizations (32) and quisqualate-stimulated release of [^{3}H]γ-aminobutyric acid from cultured neurons (23), this antagonist was ineffective at reducing the oscillating current evoked by quisqualate, ibotenate, and L-glutamate in oocytes (Fig. 10; Table 1). The oscillating current produced by ibotenate (Fig. 10) and L-glutamate (data not shown) was unmasked after the smooth current had been blocked by 10 μM CNQX.

Sources of Variability in the Measurements. The pharmacological parameters reported here were reproducible over three separate mRNA preparations and oocytes obtained from

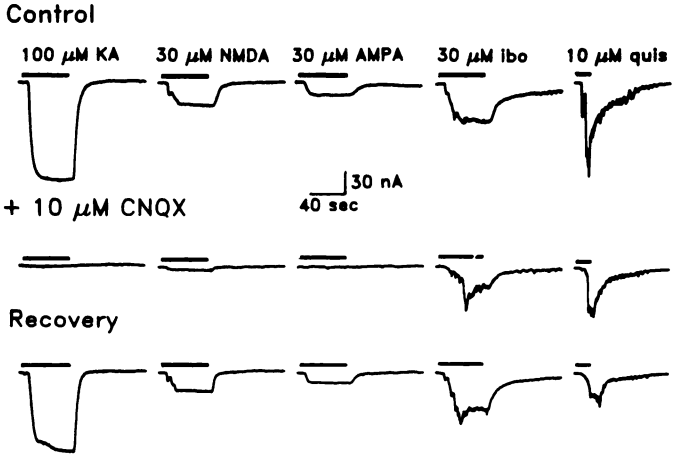

Fig. 10. The effect of 10 μM CNQX on currents elicited by various agonists. Examples of inward currents (holding potential = −60 mV) induced by the application of the agonists for the time denoted by the *bars*, under control conditions (*top*), in the presence of 10 μM CNQX (*middle*), and 10 min after the washout of CNQX (*bottom*) in the same mRNA-injected oocyte. Note that CNQX blocked the responses elicited by agonists of the NMDA and non-NMDA receptors but has little effect on the oscillating current evoked by ibotenate or quisqualate. Glycine was 3 μM throughout.

TABLE 1
Effects of CNQX on agonist currents

Receptor	Agonist[a]	Inhibition by 10 μM CNQX[b]
		%
NMDA[c]	NMDA	72 ± 4
	L-Glutamate	60 ± 3
	L-Aspartate	72 ± 2
	D-Aspartate	77 ± 4
	Ibotenate	0 ± 9
Non-NMDA	Kainate	98 ± 1
	AMPA	87 ± 5
Oscillating	Quisqualate	29 ± 12

[a] Agonists were tested at approximately EC_{50} concentrations.
[b] The maximum response amplitude was used to determine the per cent inhibition. Often the peak inward currents caused by activation of the oscillating current were large although they did not remain steady. The desensitization of the quisqualate response was partially corrected for by using the mean amplitudes of the first agonist response and the recovery as the control response amplitude. (n = 4 for each agonist).
[c] NMDA receptors were studied in the presence of 3 μM glycine and the absence of Mg^{2+}.

six donor frogs. The data obtained were normally distributed about the means as illustrated for kainate EC_{50} and kainate/CNQX pA_2 in Fig. 11. Variability in these estimates, although small, was probably not due to actual differences in the biological properties of kainate-activated receptors or to multiple quisqualate/kainate receptors. Propagation of random errors (33) associated with repeated pipetting of stock solutions and errors associated with measuring the response amplitudes combined to account for approximately two thirds of the variability in kainate EC_{50} measurements. This suggests that there is only limited variation in the pharmacological properties of the receptors expressed in different oocytes. Thus, the posttranslational processing and assembly of the receptor proteins are likely to be quite similar among the population of oocytes used in these experiments.

Discussion

The differential sensitivity to Mg^{2+}, the desensitization or rundown of NMDA but not kainate currents, and the effects of

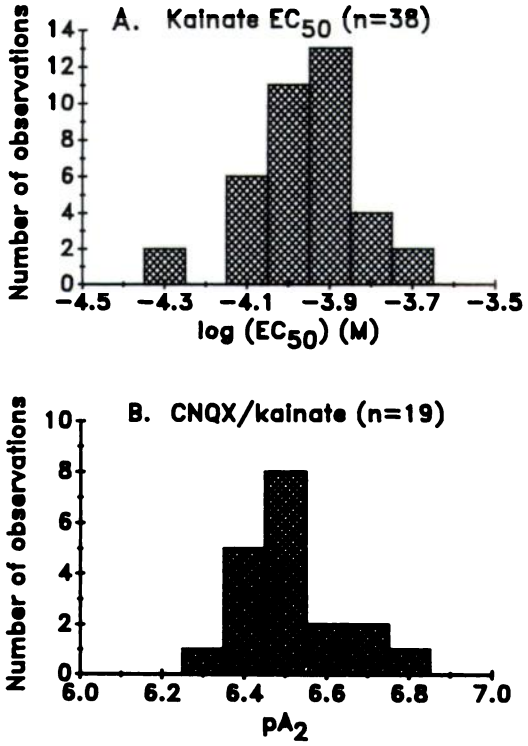

Fig. 11. The kainate EC_{50} and the pA_2 of CNQX versus kainate are normally distributed among a population of oocytes. A, The frequency distribution of kainate EC_{50} determined in 38 oocytes. The EC_{50} was determined from the fit of full concentration-response curves to the logistic equation (see Materials and Methods) or from EC_{50} estimates determined from three-point concentration-response curves constructed during Schild analyses. The mean EC_{50} in these 38 cells was 87.1 μM (95% confidence interval, 79.0–96.0 μM). B, A frequency distribution determined from 19 separate determinations of the CNQX pA_2 against kainate-evoked currents.

glycine (25, 27, 31) imply the presence of separate kainate and NMDA receptors in mRNA-injected oocytes. The data presented here regarding the effects of two antagonists that have widely different actions on NMDA- and kainate-evoked currents demonstrate that the receptors mediating NMDA and kainate currents in oocytes are pharmacologically distinct.

NMDA receptors. In neuronal preparations D-APV (7, 9, 15) and DL-APV (8, 14, 16) exert a potent and competitive antagonism of NMDA-evoked depolarizations. The data reported here concerning the effects of D-APV on NMDA receptors expressed in oocytes confirm and extend these results. Of the three neuronal studies in which the variance of the pA_2 was reported, two found DL-APV pA_2 values, 5.00 (95% confidence interval; 4.79–5.31) (16) and 4.92 ± 0.02 (14), that appeared to be significantly less potent than the value obtained in oocytes (5.87 ± 0.043), whereas the other estimate, 5.84 ± 0.01 (8), is essentially in agreement with the oocyte data. The pA_2 values reported for D-APV in neuronal preparations (average pA_2 = 5.40) also suggest that it might be slightly less potent in neurons than in oocytes (7, 9, 15). However, the latter three studies do not report variance of the estimates, making it impossible to determine whether the differences are real. Moreover, discrepancies between oocytes and neuronal data may be due to technical problems that complicate interpretation of pharmacological analysis in neuronal preparations. The complex structure of neuronal tissue may result in diffusion barriers and uptake systems that preclude knowledge of drug concentrations

in equilibrium with receptors. Slow diffusion of antagonists into tissue can generate Schild regressions with slopes of unity but shifted to the right of the actual pA_2 (34). No such barriers are present in oocytes. Additionally, the actions of endogenous substances that modulate the activity of NMDA receptors (e.g., Mg^{2+}, Zn^{2+}, and glycine) introduce additional uncertainties in interpreting pharmacological results in intact neural tissue. The concentrations of Mg^{2+}, glycine, and Zn^{2+} might change over the course of an experiment, altering the response characteristics of the tissue in uncontrollable ways. The rapid perfusion of individual defolliculated oocytes alleviates these problems because the composition of the bathing solution can be controlled and released substances (if any) are rapidly washed out.

Numerous similarities between the properties of NMDA receptors in neurons and oocytes further support the contention that the potency of D-APV reported here reflects its potency at neuronal NMDA receptors. The potencies of antagonists determined with Schild analysis should match their affinities in radioligand binding studies (35). The average K_i for inhibition by D-APV of radioligand binding to NMDA receptors in neuronal membrane preparations, 1.4 μM (7, 15, 36–42), corresponds closely to the D-APV K_B at oocyte NMDA receptors (1.35 μM). The voltage independence of the effect of D-APV in oocytes (26) is similar to that in neurons (43). In other respects, oocyte NMDA receptors appear similar to neuronal NMDA receptors. The relative potencies of NMDA agonists as well as the effects of Mg^{2+} (26), glycine (25, 31), and Zn^{2+} (31) in oocytes are all very similar to those found in neuronal preparations. The rundown of the NMDA response in oocytes is also seen in neurons (30). In neurons this effect may be due to modulation of NMDA receptor activity by phosphorylation (30). Although the Ca^{2+} permeability of the oocyte NMDA channel has not been tested, the available evidence supports the conclusion that the properties of the oocyte NMDA receptor are indistinguishable from those of its neuronal counterpart. Consequently, the generalization of the results reported here to neuronal NMDA receptors appears justified.

The properties of currents evoked by L-aspartate in mRNA-injected oocytes indicate that they are also mediated largely by NMDA receptors. NMDA- and L-aspartate-induced currents appear qualitatively similar, and Mg^{2+} exerts a voltage-dependent block of both responses (26). Stronger evidence that L-aspartate and NMDA act at the same receptor in oocytes is provided by the finding that the D-APV Schild regression for L-aspartate is identical to that obtained for NMDA. Remarkably, NMDA and L-aspartate at concentrations well above 1 mM appear to be selective for NMDA receptors in oocytes, because the D-APV Schild plots are linear and have a slope of unity up to at least 10 mM NMDA and 6 mM aspartate. Significant effects on other receptors coupled to ion channels would likely be manifested in nonlinearity of the Schild plot (34). The high degree of selectivity exhibited by L-aspartate in oocytes and in neurons (44) is in sharp contrast to the mixed actions of L-glutamate in oocytes (26) and in neurons (44). Thus, these results raise the possibility that the synaptic target of neurons releasing L-aspartate as a neurotransmitter would be exclusively NMDA receptors.

The effect of CNQX on NMDA-evoked currents in oocytes also appears similar to that found in neurons. In oocytes CNQX exerts a noncompetitive block of NMDA responses and a mixed competitive-noncompetitive block at the glycine site on NMDA receptors. Recent results by Birch *et al.* (45) are consistent with an action of CNQX on this glycine site in an *in vitro* rat spinal cord preparation. Kemp *et al.* (21) also reported that a structurally similar compound, 7-chlorokynurenic acid, is a competitive glycine antagonist, and the effects of kynurenate itself are consistent with this mode of action (43). It is very interesting that quinoxalines and similar structures are competitive antagonists of both quisqualate/kainate receptors and the glycine site of NMDA receptors. The possibility that these two ligand binding sites may share structural features in under further investigation. The noncompetitive component of the block of glycine effects could be due to an additional action of CNQX, perhaps a non-voltage-dependent block of the NMDA channel, similar to the effect of Zn^{2+} (46).

Reports that CNQX competitively blocked NMDA-induced responses in cortical cultures (23) and slices (47) might be accounted for by spare receptors. Spare receptors, if present in neuronal preparations, or release of endogenous agonists evoked by applied compounds could obscure the noncompetitive properties of CNQX in neurons (23, 47) over the limited antagonist concentration range studied (34).

Quisqualate/kainate receptors. In agreement with its effects in neurons (23, 32), CNQX is a potent competitive antagonist of kainate-induced currents in oocytes. Although separate kainate and quisqualate/AMPA binding sites exist (37, 48), evidence obtained from electrophysiological studies has failed to differentiate between these two EAA receptors. Kainate binds to neuronal membranes with a K_d of 5–10 nM (49) but 1000-fold higher concentrations of kainate are required to open cation channels in neurons (2, 4, 5, 27, 50, 51) and in oocytes (26). Furthermore, there are significant interactions between currents evoked by kainate and quisqualate in neuronal preparations (51–53) and in oocytes (26), and the agonist potency ratios for this current match those expected for binding to the AMPA/quisqualate site but not the high affinity kainate site (26). The potency of CNQX against kainate currents in oocytes is also consistent with the receptor mediating the non-NMDA current being the AMPA/quisqualate receptor identified by binding studies. The K_B estimated in oocytes (295 nM) is similar to the CNQX IC_{50} for inhibition of [^{3}H]AMPA binding (275 nM). In contrast, CNQX inhibits high affinity [^{3}H]kainate binding with a IC_{50} of 1.7 μM (32). In oocytes, kainate appears to be a quisqualate receptor agonist with relatively low potency and much less tendency to desensitize (cf. ref. 51) than either quisqualate or AMPA. Thus, the available evidence supports the hypothesis that much or all of the depolarizing action of kainate, in neurons and in oocytes, is due to activation of the receptor corresponding to the quisqualate/[^{3}H]AMPA binding site. Fletcher *et al.* (47) reached a similar conclusion from studies in rat neocortical slices.

D-APV also blocks the currents mediated by kainate, but with low potency. The ratio of D-APV potencies at blocking NMDA- and kainate-induced currents in oocytes, 295, is similar to that reported by Jones *et al.* (19), 452. Because relatively high concentrations of D-APV were necessary to block kainate responses, possible effects of contaminants must be considered. The optical purity of the D-APV used in these experiments was reported by the manufacturer to be 96%; thus, there may have been a significant concentration of L-APV (20–160 μM) present during the Schild analysis for kainate. It is possible that L-

APV or another contaminant may have affected the slope of the regression and the pA_2 estimate. This should have resulted in a nonlinear Schild regression that might have gone undetected because of the relatively narrow range of antagonist concentrations that we were able to test. The large difference between the D-APV pA_2 values for kainate and NMDA indicate that the weak block by D-APV of kainate currents is not due to nonspecific actions of kainate on NMDA receptors. Furthermore, the linear Schild plot generated for kainate with CNQX indicates that kainate is selective for the non-NMDA receptor in oocytes at concentrations above 10 mM.

The results of these and previous (25–27) experiments provide a basis for further quantitative studies of EAA receptors expressed in oocytes. For example, the pharmacological properties of receptors translated by mRNA expressed in different brain regions or developmental ages can be compared. The oocyte system permits the degree of quantitation necessary for detecting small differences in receptor properties, making it useful for the characterization of new compounds that act on the agonist binding sites or other modulatory sites associated with NMDA and non-NMDA EAA receptors.

Acknowledgments

We thank Dr. Tage Honore for the generous gift of CNQX and Dr. Alan Foster for comments on the manuscript.

References

1. Watkins, J. C. and R. H. Evans. Excitatory amino acid transmitters. *Annu. Rev. Pharmacol. Toxicol.* **21**:165–204 (1981).
2. Ascher, P., and L. Nowak. Quisqualate and kainate activated channels in mouse central neurones in culture. *J. Physiol. (Lond.)* **399**:227–246 (1988).
3. Ascher, P., P. Bregestovski, and L. Nowak. *N*-Methyl-D-aspartate activated channels of mouse central neurones in magnesium free solutions. *J. Physiol. (Lond.)* **399**:207–226 (1988).
4. Cull-Candy, S. G., and M. M. Usowicz. Multiple-conductance channels activated by excitatory amino acids in cerebellar neurons. *Nature (Lond.)* **325**:525–528 (1987).
5. Jahr, C. E., and C. F. Stevens. Glutamate activates multiple single channel conductances in hippocampal neurons. *Nature (Lond.)* **325**:522–525 (1987).
6. Johnson, J. W., and P. Ascher. Glycine potentiates the NMDA response in cultured mouse brain neurons. *Nature (Lond.)* **325**:529–531 (1987).
7. Davies, J., R. H. Evans, P. L. Herrling, A. W. Jones, H. J. Olverman, P. Pook, and J. C. Watkins. CPP, a potent and selective NMDA antagonist: depression of central neuron responses, affinity for [^{3}H]D-AP5 binding sites on brain membranes and anticonvulsant activity. *Brain Res.* **382**:169–173 (1986).
8. Evans, R. H., A. A. Francis, A. W. Jones, D. A. S. Smith, and J. C. Watkins. The effects of a series of ω-phosphonic α-carboxylic amino acids on electrically evoked and excitant amino acid-induced responses in isolated spinal cord preparations. *Br. J. Pharmacol.* **75**:65–75 (1982).
9. Harrison, N. L., and M. A. Simmonds. Quantitative studies on some antagonists of *N*-methyl-D-aspartate in slices of rat cerebral cortex. *Br. J. Pharmacol.* **84**:381–391 (1985).
10. Herrling, P. L. Pharmacology of the corticocaudate excitatory postsynaptic potential in the cat: evidence for its mediation by quisqualate- or kainate-receptors. *Neuroscience* **14**:417–426 (1985).
11. Huettner, J. E., and B. P. Bean. Block of *N*-methyl-D-aspartate-activated current by the anticonvulsant MK-801: selective binding to the open channel. *Proc. Natl. Acad. Sci. USA* **85**:1307–1311 (1988).
12. MacDonald, J. F., Z. Miljkovic, and P. Pennefather. Use-dependent block of excitatory amino acid currents in cultured neurons by ketamine. *J. Neurophysiol.* **58**:251–266 (1987).
13. Nowak, L., P. Bregestovski, P. Ascher, P. Herbert, and A. Prochiantz. Magnesium gates glutamate-activated channels in mouse central neurones. *Nature (Lond.)* **307**:462–465 (1984).
14. Burton, N. R., D. A. S. Smith, and T. W. Stone. A quantitative pharmacological analysis of some excitatory amino acid receptor in the mouse neocortex *in vitro*. *Br. J. Pharmacol.* **93**:693–701 (1988).
15. Foster, A. C., J. A. Kemp, S. Grimwood, E. H. F. Wong, and G. E. Fagg. Investigations of *N*-methyl-D-aspartate receptors using radioligand binding techniques, in *Excitatory Amino Acid Transmission* (T. P. Hicks, D. Lodge, and H. McLennen, eds.). Alan R. Liss, New York, 107–114 (1987).
16. Wheatley, P. L., and K. J. Collins. Quantitative studies of *N*-methyl-D-aspartate, 2-amino-5-phosphonovalerate and *cis*-2,3-piperidine dicarboxylate interactions on the neonatal rat spinal cord *in vitro*. *Eur. J. Pharmacol.* **121**:257–263 (1986).
17. Perkins, M. N., and T. W. Stone. Pharmacology and regional variations of quinolinic acid evoked excitation in the rat central nervous system. *J. Pharmacol. Exp. Ther.* **226**:551–557 (1983).
18. Davies, J., and J. C. Watkins. Diferentiation of kainate and quisqualate receptors in the cat spinal cord by selective antagonism with D- (and L)-glutamylglycine. *Brain Res.* **206**:172–177 (1981).
19. Jones, A. W., D. A. S. Smith, and J. C. Watkins. Structure-activity relations of dipepetide antagonists of excitatory amino acids. *Neuroscience* **13**:573–581 (1984).
20. Evans, R. H., S. J. Evans, P. C. Pook, and D. C. Sunter. A comparison of excitatory amino acid antagonists acting at primary afferent C fibres and motoneurones of the isolated spinal cord of the rat. *Br. J. Pharmacol.* **91**:531–537 (1987).
21. Kemp, J. A., A. C. Foster, P. D. Leeson, T. Priestley, R. Tridgett, L. L. Iversen, and G. N. Woodruff. 7-Chlorokynurenic acid is a selective antagonist at the glycine site of the *N*-methyl-D-aspartate receptor complex. *Proc. Nat. Acad. Sci. USA* **85**:6547–6550 (1988).
22. Ganong, A. H., A. W. Jones, J. C. Watkins, and C. W. Cotman. Parallel antagonism of synaptic transmission and kainate/quisqualate responses in the hippocampus by piperazine-2,3-dicarboxylic acid analogs. *J. Neurosci.* **9**:930–937 (1986).
23. Drejer, J., and T. Honore. New quinoxalinediones show potent antagonism of quisqualate response in cultured mouse cortical neurons. *Neurosci. Lett.* **87**:104–108 (1988).
24. Garthwaite, J. Cellular uptake disguises action of L-glutamate on *N*-methyl-D-aspartate receptors. *Br. J. Pharmacol.* **85**:297–307 (1985).
25. Kleckner, N. W., and R. Dingledine. Requirement for glycine in activation of NMDA-receptors expressed in *Xenopus* oocytes. *Science (Wash. D. C.)* **241**:835–837 (1988).
26. Verdoorn, T. A., and R. Dingledine. Excitatory amino acid receptors expressed in *Xenopus* oocytes: agonist pharmacology. Mol. Pharmacol. **34**:298–307 (1988).
27. Verdoorn, T. A., N. W. Kleckner, and R. Dingledine. Expression of rat brain *N*-methyl-D-aspartate receptors in *Xenopus* oocytes. *Science (Wash. D. C.)* **238**:1114–1116 (1987).
28. Verdoorn, T. A., and R. Dingledine. Antagonist pharmacology of excitatory amino acid receptors expressed in *Xenopus* oocytes. *Soc. Neurosci. Abstr.* **14**:1193 (1988).
29. Arunlakshana, O., and H. O. Schild. Some quantitative uses of drug antagonists. *Br. J. Pharmacol.* **14**:48–57 (1959).
30. Mody, I., M. W. Salter, and J. F. MacDonald. Requirement of NMDA receptor/channels for intracellular high-energy phosphates and the extent of intraneuronal calcium buffering in cultured mouse hippocampal neurons. *Neurosci. Lett.* **93**:73–75 (1988).
31. Kushner, L., J. Lerma, R. S. Zukin, and M. V. L. Bennett. Coexpression of *N*-methyl-D-aspartate and phencyclidine receptors in *Xenopus* oocytes injected with rat brain mRNA. *Proc. Natl. Acad. Sci. USA* **85**:3250–3254 (1988).
32. Honore, T., S. N. Davies, J. Drejer, E. J. Fletcher, P. Jacobsen, D. Lodge, and F. E. Nielsen. Quinoxalinediones: potent competitive non-NMDA glutamate receptor antagonists. *Science (Wash. D. C.)* **241**:701–703 (1988).
33. Skoog, D. A., and D. M. West. *Fundamentals of Analytical Chemistry*. Saunders College, Philadelphia (1976).
34. Kenakin, T. P. *Pharmacologic Analysis of Drug-Receptor Interaction*. Raven Press, New York (1987).
35. Furchgott, R. F. Pharmacological characterization of receptors: its relation to radioligand-binding studies. *Fed. Proc. Am. Soc. Exp. Biol.* **37**:115–120 (1978).
36. Foster, A. C., and G. E. Fagg. Acidic amino acid binding sites in mammalian neuronal membranes: their characteristics and relationship to synaptic receptors. *Brain Res. Rev.* **7**:103–164 (1984).
37. Greenamyre, J. T., J. M. M. Olsen, J. B. Penney, and A. B. Young. Autoradiographic characterization of *N*-methyl-D-aspartate-, quisqualate- and kainate-sensitive glutamate binding sites. *J. Pharmacol. Exp. Ther.* **233**:254–263 (1985).
38. Monaghan, D. T., D. Yao, and C. W. Cotman. L-[^{3}H]Glutamate binds to kainate-, NMDA- and AMPA-sensitive binding sites: an autoradiographic analysis. *Brain Res.* **340**:378–383 (1985).
39. Monahan, J. B., and J. Michel. Identification and characterization of an *N*-methyl-D-aspartate-specific L-[^{3}H]glutamate recognition site in synaptic plasma membranes. *J. Neurochem.* **48**:1699–1708 (1987).
40. Murphy, D. E., J. Schneider, C. Boehm, J. Lehman, and M. Williams. Binding of [^{3}H]3-(2-carboxypiperazin-4-yl)propyl-1-phosphonic acid to rat brain membranes: a selective, high affinity ligand for *N*-methyl-D-aspartate receptors. *J. Pharmacol. Exp. Ther.* **240**:778–784 (1987).
41. Olverman, H. J., A. W. Jones, and J. C. Watkins. L-Glutamate has a higher affinity than other amino acids for [^{3}H]-D-APV binding sites in rat brain membranes. *Nature (Lond.)* **307**:460–462 (1984).
42. Olverman, H. J., D. T. Monaghan, C. W. Cotman, and J. C. Watkins. [^{3}H] CPP, a new competitive ligand for NMDA receptors. *Eur. J. Pharmacol.* **131**:161–162 (1986).
43. Mayer, M. L., and G. L. Westbrook. Mixed agonist action of excitatory amino acids on mouse spinal cord neurones under voltage clamp. *J. Physiol. (Lond.)* **354**:29–53 (1984).

44. Mayer, M. L., G. L. Westbrook, and L. Vyklicky. Sites of antagonist action on *N*-methyl-D-aspartic acid receptors studied using fluctuation analysis and a rapid perfusion technique. *J. Neurophysiol.* **60**:645–663 (1988).
45. Birch, P. J., C. J. Grossman, and A. G. Hayes. 6,7-Dinitro-quinoxaline-2,3-dion and 6-nitro,7-cyano-quinoxaline-2,3-dion antagonize responses to NMDA via an action at the strychnine-insensitive glycine receptor. *Br. J. Pharmacol.*, **156**:177–180 (1988).
46. Westbrook, G. L., and M. L. Mayer. Micromolar concentrations of Zn^{++} antagonize NMDA and GABA responses of hippocampal neurons. *Nature (Lond.)* **328**:640–643 (1987).
47. Fletcher, E. J., D. Martin, J. A. Aram, D. Lodge, and T. Honore. Quinoxalinediones selectively block quisqualate and kainate receptors and synaptic events in rat neocortex and hippocampus and frog spinal cord *in vitro*. *Br. J. Pharmacol.* **95**:585–597 (1988).
48. Monaghan, D. T., and C. W. Cotman. Anatomical organization of NMDA, kainate, and quisqualate receptors, in *Excitatory Amino Acids* (P. J. Roberts, J. Storm-Mathisen, and H. F. Bradford, eds.). Macmillan, London, 279–299 (1986).
49. London, E. D., and J. T. Coyle. Specific binding of [^{3}H]kainate to receptor sites in rat brain. *Mol. Pharmacol.* **15**:492–505 (1979).
50. Kiskin, N. I., O. A. Krishtal, and A. Y. Tsyndrenko. Excitatory amino acid receptors in hippocampal neurons: kainate fails to desensitize them. *Neurosci. Lett.* **63**:225–230 (1986).
51. O'Brien, R. J., and G. O. Fischbach. Characterization of excitatory amino acid receptors expressed by embryonic chick motoneurons *in vitro*. *J. Neurosci.* **6**:3275–3283 (1986).
52. Aizenmann, E., M. P. Froech, and S. A. Lipton. Responses mediated by excitatory amino acid receptors in solitary retinal ganglion cells from rat. *J. Physiol. (Lond.)* **396**:75–91 (1988).
53. Ishida, A. T., and J. Neyton. Quisqualate and L-glutamate inhibit retinal horizontal-cell response to kainate. *Proc. Natl. Acad. Sci. USA* **82**:1837–1841 (1985).

Send reprint requests to: Raymond Dingledine, Dept. of Pharmacology, FLOB CB 7365, University of North Carolina, Chapel Hill, NC 27599.